Room Temperature Phosphorescence from a Benzothiophene-based N-B-N Multi-Resonance Core

*Durai Karthik,[a,b‡] Abhishek Kumar Gupta,[a‡] and Eli Zysman-Colman[a]**

[a]Organic Semiconductor Centre, EaStCHEM School of Chemistry, University of St Andrews, St Andrews, UK, KY16 9ST. E-mail: eli.zysman-colman@st-andrews.ac.uk

[b]Current address: Department of Chemistry, SRM Institute of Science and Technology, Kattankulathur – 603203, Tamil Nadu, India

‡ These authors contributed equally.

SUPPORTING INFORMATION

Table of Contents

General methods

General Synthetic Procedures. All reagents and solvents were obtained from commercial sources and used as received. Air-sensitive reactions were performed under a nitrogen atmosphere using Schlenk techniques, no special precautions were taken to exclude air or moisture during work-up and crystallisation. Flash column chromatography was carried out using silica gel (Silica-P from Silicycle, 60 Å, 40-63 μm). Analytical thin-layer-chromatography (TLC) was performed with silica plates with aluminum backings (250 μm with F-254 indicator). TLC visualization was accomplished by 254/365 nm UV lamp. ^{1}H NMR spectra were recorded on a Bruker Advance spectrometer (400 or 500 MHz for ^{1}H and 100 or 125 for ^{13}C). The following abbreviations have been used for multiplicity assignments: "s" for singlet, "d" for doublet, and "dd" for doublet of doublet. ^{1}H NMR spectra were referenced to residual solvent peaks with respect to TMS (δ = 0 ppm). High performance liquid chromatography (HPLC) was conducted on a Shimadzu LC-40 HPLC system. HPLC traces were performed using a Shim-pack GIST 3μm C18 reverse phase analytical column using THF:water (8:2) as mobile phase. Melting point was measured using open-ended capillaries on an Electrothermal 1101D Mel-Temp apparatus and are uncorrected. High-resolution mass spectrometry (HRMS) was performed using microTOF at the University of Edinburgh Mass Spectrometry Facility. TGA measurements were conducted on a Netzsch STA449C with a heating rate of 10 °C/min under a nitrogen atmosphere. The samples were heated from 19 to 700 °C and the thermal decomposition temperature (T_d) was determined at a threshold of 5 % weight loss.

Photophysical measurements. Optically dilute solutions of concentrations on the order of 10^{-5} to 10^{-6} M were prepared in spectroscopic or HPLC grade solvents for absorption and emission analyses. Absorption spectra were recorded at room temperature on a Shimadzu UV-2600 double beam spectrophotometer with a 1 cm quartz cuvette. Molar absorptivity determination was verified by linear regression analysis of values obtained from at least five independent solutions at varying concentrations with absorbance ranging from 0.354 to 1.411 for **BT-DBIP**. Steady-state emission and excitation spectra and

time-resolved emission decays were recorded at 298 K using an Edinburgh Instruments FS5 spectrofluorometer. Samples were excited at 374 nm for steady-state measurements and at 375 nm for time-resolved measurements.

ΔE_{ST} *measurement in solution*. An open 150 mL EPR Dewar was used for the singlet-triplet energy gap (ΔE_{ST}) measurements of solution samples. The ΔE_{ST} was determined by recording the steady-state photoluminescence and delayed emission spectra of the emitter in 2-MeTHF glass at 77 K. The delayed emission spectra were measured after 1 ms excitation of the Xenon flashlamp operating at 100 Hz with an exposure time of 9 ms. The singlet (S_1) and triplet (T_1) energies were then determined from the corresponding onsets of steady-state and delayed emission spectra at 77 K and ΔE_{ST} calculated by using the equation $\Delta E_{ST} = S_1 - T_1$.

Photophysical measurement in the solid state. The film for solid state photophysical studies was prepared by spin-coating of 2 wt% emitter in a chlorobenzene solution of *N,N'*-dicarbazolyl-3,5-benzene (mCP) host, on cleaned sapphire substrates. The photophysical properties of the film samples were measured using an Edinburgh Instruments FS5 fluorimeter.

Photoluminescence quantum yields *measurements in solution*

Photoluminescence quantum yields (Φ_{PL}) for solutions were determined using the optically dilute method[1] in which four sample solutions with absorbances of ca. 0.10, 0.075, 0.050 and 0.025 at 347 nm were used. The Beer-Lambert law was found to remain linear across the concentrations of the solutions. For each sample, linearity between absorption and emission intensity was verified through linear regression analysis with the Pearson regression factor (R^2) for the linear fit of the data set surpassing 0.9. Individual relative quantum yield values were calculated for each solution and the values reported represent the slope obtained from the linear fit of these results. The Φ_{PL} was determined using the equation $\Phi_{PL} = (\Phi_r * \frac{A_r}{A_s} * \frac{I_s}{I_r} * \frac{n_s^2}{n_r^2})$, where A stands for the absorbance at the excitation wavelength (λ_{exc}: 347 nm), I is the integrated area under the corrected emission curve and n is the refractive index of the solvent with the subscripts "s" and "r" representing sample and reference respectively. Φ_r is the absolute

PL quantum yield of the external reference, quinine sulfate (Φ_r = 54.6% in 0.5 *N* H_2SO_4).[2, 3] The experimental uncertainty in the Φ_{PL} is conservatively estimated to be 10%, though we have found that statistically we can reproduce Φ_{PL} values to within 3% relative error.

Photoluminescence quantum yields (Φ_{PL}) of the thin film. An integrating sphere (Edinburgh Instruments FS5, SC30 module) was employed for the photoluminescence quantum yield measurements of the thin film samples. The Φ_{PL} of the films were then measured in air and in N_2, the latter by purging the integrating sphere with N_2 gas flow for 2 min.

Steady-state emission and time-resolved PL decay of thin film samples. Steady-state PL spectra and time-resolved PL decays were recorded at 300, 200, and 77 K using an Edinburgh Instruments FS5 fluorimeter in an oxygen-free atmosphere. Oxygen-free samples were obtained by placing the sample inside a cold finger cryostat (Oxford Instruments) under vacuum ($< 8 \times 10^{-4}$ mbar). All the samples for the steady-state measurements were excited at 340 nm using a Xenon lamp, while the samples for the time-resolved measurements were excited at 375 nm using a pico-second laser (PicoQuant, LDH-D-C-375) driven by a laser driver (PDL 800-D). PL decays were measured using time-correlated single photon counting (TCSPC) mode and multi-channel scaling (MCS). For quantify the long-delayed lifetime, the samples were excited at 340 nm by using a 5 W pulsed Xenon flashlamp under vacuum. For ΔE_{ST}, all samples were loaded inside a cold finger cryostat (Oxford Instruments) and samples were placed under vacuum. The S_1, T_1, and ΔE_{ST} energies of films were determined using the same methodology as for measurements in the glass at 77 K (*vide-supra*) after excitation the sample at 340 nm.

Fitting of time-resolved luminescence measurements: Time-resolved PL measurements were fitted to a sum of exponentials decay model, with chi-squared (χ^2) values between 1 and 2, using the EI software. Each component of the decay is assigned a weight, (w_i), which is the contribution of the emission from each component to the total emission.

The average lifetime was then calculated using the following:

- Two exponential decay model:

$$\tau_{AVG} = \tau_1 w_1 + \tau_2 w_2$$

with weights defined as $w_1 = \frac{A1\tau_1}{A1\tau_1 + A2\tau_2}$ and $w_2 = \frac{A2\tau_2}{A1\tau_1 + A2\tau_2}$ where A1 and A2 are the preexponential-factors of each component.

Electrochemistry measurements. Cyclic Voltammetry (CV) analysis was performed on an Electrochemical Analyzer potentiostat model 620E from CH Instruments at a sweep rate of 50 mV/s. Differential pulse voltammetry (DPV) was conducted with an increment potential of 0.004 V and a pulse amplitude, width, and period of 50 mV, 0.05, and 0.5 s, respectively. Samples were dissolved in dichloromethane (DCM) and were degassed by sparging with DCM-saturated nitrogen gas for 5 minutes prior to measurements. All measurements were performed using 0.1 M DCM solution of tetra-*n*-butylammonium hexafluorophosphate ([^{n}Bu$_4$N]PF$_6$]). An Ag/Ag$^+$ electrode was used as the reference electrode while a platinum electrode and a platinum wire were used as the working electrode and counter electrode, respectively. The HOMO energy was determined using the relation $E_{HOMO} = -(E_{ox} + 4.8)$ eV,[4, 5] where E_{ox} is the anodic peak potential calculated from DPV related to Fc/Fc$^+$. The LUMO energy was calculated using the relation $E_{LUMO} = E_{HOMO} - E_{opt}$. The optical gap ($E_{opt}$) was calculated from the intersection point between the normalized absorption and emission spectra (Figure **S15**).

Quantum chemical calculations. All ground state optimizations have been carried out at the Density Functional Theory (DFT) level with Gaussian 16[6] using the PBE0[7] functional and the 6-31G(d,p) basis set.[8] Excited-state calculations have been performed at Tamm-Dancoff approximation DFT (TDA-DFT)[9, 10] using the same functional and basis set as for ground state geometry optimization. Spin-orbit coupling matrix elements (x) were calculated based on the optimized ground state geometry. Molecular orbitals were visualized using GaussView 6.0.[11] Calculations were submitted and processed using the Digichem (version 6) software package,[12, 13] which incorporates a number of publicly available software libraries, including: cclib[14] for parsing of result files, VMD[15] and Tachyon[16] for 3D rendering, Matplotlib[17] for the plotting of graphs, Open Babel[18] and Pybel[19] for file interconversion, and PySOC[20] for the calculation of spin-orbit coupling. The Huang–Rhys factors were calculated using the optimized geometries of the ground (S_0) and excited (S_1) states at the PBE0/6-31G(d,p) level of theory. The reorganization energies of the emitter were subsequently evaluated using the DUSHIN program based on the vibrational normal-mode analysis of these optimized structures. [21]

Synthesis

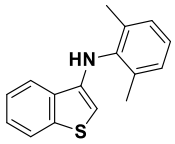

***N*-(2,6-dimethylphenyl)benzo[b]thiophen-3-amine (1)**

A Schlenk flask under nitrogen was charged with 3-bromobenzo[*b*]thiophene (5.00 g, 23.46 mmol, 1.0 equiv.), 2,6-dimethylaniline (2.84 g, 23.46 mmol, 1.0 equiv.), sodium *tert*-butoxide (4.07 g 46.92 mmol, 2.0 equiv.), [^{t}Bu$_3$PH]BF$_4$ (0.12 g, 0.71 mmol, 0.03 equiv.) and Pd$_2$(dba)$_3$ (0.19 g, 0.35 mmol, 0.015 equiv.) was added in toluene (30 mL) and heated at 100 °C under inert atmosphere for 2 h. The mixture was cooled, diluted with EtOAc (200 mL) and then filtered through a pad of celite. The organic fraction was concentrated under reduced pression and adsorbed on alumina. The compound was purified by alumina column chromatography using hexane as the eluant. Dark brown crystalline solid. **Yield:** 49% (2.90 g). **Mp**: 133 - 135 °C. **R$_f$:** 0.55 (hexane). **^{1}H NMR (400 MHz, DMSO) δ (ppm):** 8.15 – 8.13 (m, 1H), 7.87 – 7.84 (m, 1H), 7.43 – 7.35 (m, 3H), 7.15 – 7.13 (m, 2H), 7.09 – 7.05 (m, 1H), 5.49 (s, 1H), 2.18 (s, 1H). **^{13}C NMR (125 MHz, DMSO) δ (ppm)** 140.35, 140.11, 139.15, 135.37, 133.13, 128.88, 125.77, 125.07, 123.81, 123.47, 121.54, 95.21, 18.31. **HR-MS[M+H]$^+$** Calculated: 254.0998 (C$_{16}$H$_{15}$NS); Found: 254.0999.

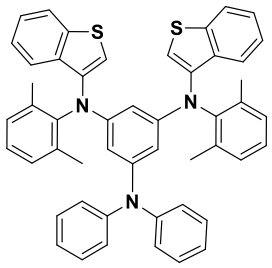

***N*1,*N*3-bis(benzo[*b*]thiophen-3-yl)-*N*1,*N*3-bis(2,6-dimethylphenyl)-*N*5,*N*5-diphenylbenzene-1,3,5-triamine (2)**

A dried Schlenk flask under nitrogen was charged with a mixture of 3,5-dichloro-*N*,*N*-diphenylaniline (1.00 g, 3.18 mmol, 1.0 equiv.), *N*-(2,6-dimethylphenyl)benzo[*b*]thiophen-3-amine (1.77 g, 7.00 mmol, 2.2 equiv.), sodium tert-butoxide (0.76 g, 7.95 mmol, 2.5 equiv.), Xphos (0.76 g, 1.59 mmol, 0.5 equiv.)

and $Pd_2(dba)_3$ (0.15 g, 0.16 mmol, 0.05 equiv.) in toluene (20 mL) was heated at 110 °C. After 18 h, the reaction mixture was allowed to cool to room temperature and filtered through silica/celite pad and washed with DCM (200 mL). The collected organic fractions were concentrated under reduced pressure. The crude mixture was purified by flash column chromatography using DCM/hexane (3/7, v/v) as eluant. Dark yellow solid. **Yield:** 84% (2.00 g). **Mp**: 150-155 °C. **R_f :** 0.35 (30 : 70 DCM : hexane). **^{1}H NMR (300 MHz, DMSO) δ (ppm):** 7.87 – 7.84 (m, 2H), 7.68 – 7.66 (m, 2H), 7.36 – 7.23 (m, 8H), 7.09 – 7.06 (m, 3H), 6.99 (t, *J* = 7.26 Hz, 2H), 6.86 (d, *J* = 7.74 Hz, 4H), 6.78 – 6.70 (m, 6H), 6.55 (d, *J* = 1.35 Hz, 2H), 1.80 (s, 12H). **^{13}C NMR (125 MHz, $CDCl_3$) δ (ppm)** 147.79, 147.10, 140.17, 136.90, 135.96, 134.79, 132.71, 130.70, 129.19, 128.73, 124.76, 124.58, 123.98, 123.30, 122.89, 122.51, 122.26, 121.29, 121.20, 121.10, 18.78. **HR-MS[M+H]$^+$** Calculated: 747.2732 ($C_{50}H_{41}N_3S_2$); Found: 747.2736.

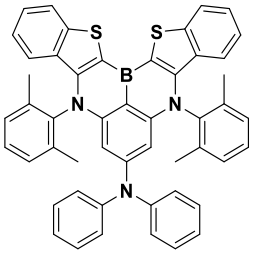

5,9-bis(2,6-dimethylphenyl)-*N*,*N*-diphenyl-5*H*,9*H*-14,15-dithia-5,9-diaza-14b-boradiindeno[2,1-*a*:1',2'-*j*]phenalen-7-amine (BT-DBIP)

To a solution of **2** (0.15 g, 0.22 mmol, 1.0 equiv.) in 1,2-dichlorobenzene (4 mL) was added boron tribromide (0.04 mL, 0.40 mmol, 1.8 equiv.) under a nitrogen atmosphere at room temperature. After stirring at 180 °C for 24 h, the reaction mixture was allowed to cool to room temperature. Then, further it was cooled to 0 °C in an ice bath and *N,N*-diisopropylethylamine (0.08 mL, 0.44 mmol, 2.0 equiv.) was added. This mixture was allowed to warm to room temperature and stirred for 2h. Then, the solvent was removed in vacuo to obtain the crude product, then, the crude was purified by column chromatography using DCM/hexane (1/3, v/v) as eluent. Yellow solid. **Yield:** 56% (93 mg). **R_f :** 0.4 (30 : 70 DCM : hexane) **Mp:** 320-323 ºC. **HPLC purity:** > 99.80% (retention time: 5.60 minutes for **BT-DBIP** employing an eluent of 8:2 THF:H_2O). **^{1}H NMR (500 MHz, $CDCl_3$) δ (ppm):** 7.66 (d, *J* = 7.45 Hz, 2H), 7.39 – 7.34 (m, 8H), 7.27 (s, 2H), 7.18 – 7.16 (m, 2H), 7.11 (t, *J* = 7.50 Hz, 2H), 7.03 (t, *J* = 7.60 Hz,

2H), 6.79 (d, J = 7.60 Hz, 4H), 6.75 ((t, J = 7.95 Hz, 2H), 5.46 (d, J = 8.65 Hz, 2H), 1.89 (s, 12H). **^{13}C NMR (125 MHz, $CDCl_3$) δ (ppm)** 151.08, 147.41, 141.43, 139.23, 138.01, 137.30, 136.40, 133.64, 129.44, 128.12, 127.23, 125.36, 124.37, 123.92, 123.74, 122.93, 122.76, 119.41, 111.48, 19.23. **HR-MS[M+H]$^+$**Calculated: 756.2673 ($C_{50}H_{39}B_1N_3S_2$); Found: 756.2649. **Elemental analysis:** Calcd for **BT-DBIP** $C_{50}H_{38}BN_3S_2$: C, 79.46; H, 5.07; N, 5.56 Found: C, 78.70; H, 5.15; N, 5.18.

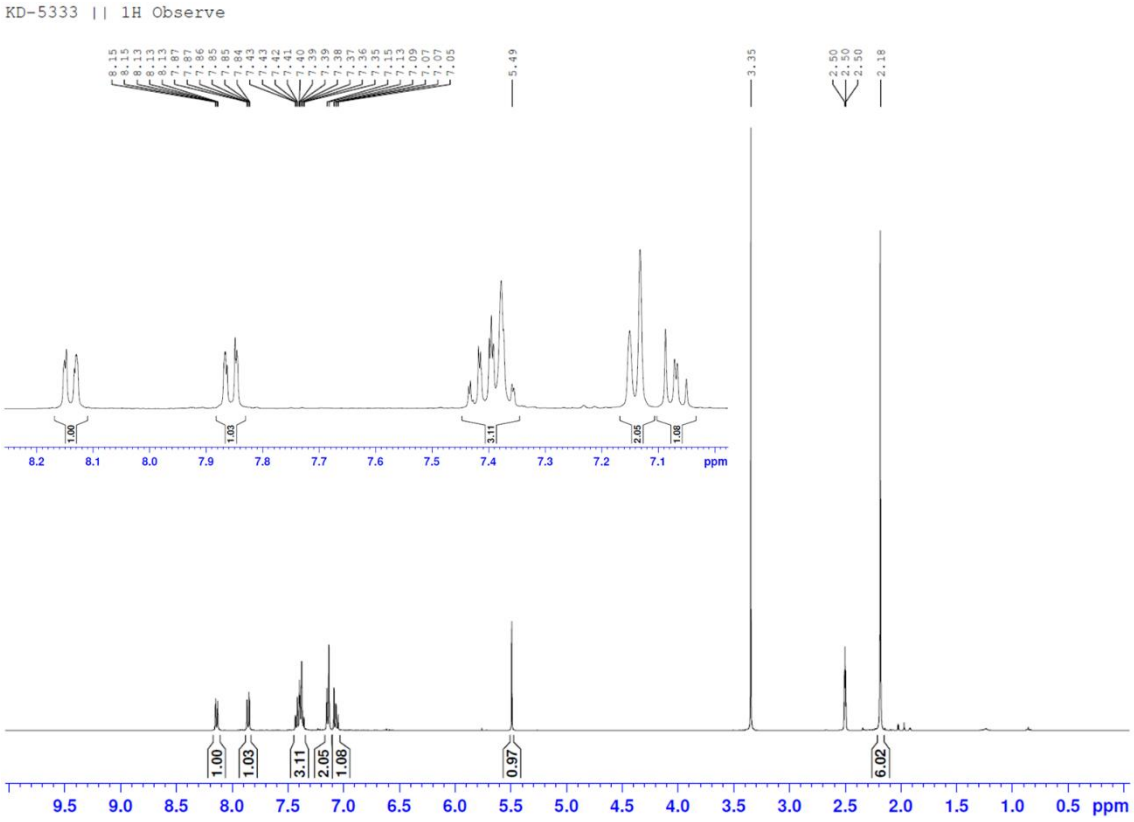

Fig. **S1**. ^{1}H NMR spectrum of **1** in DMSO-d_6.

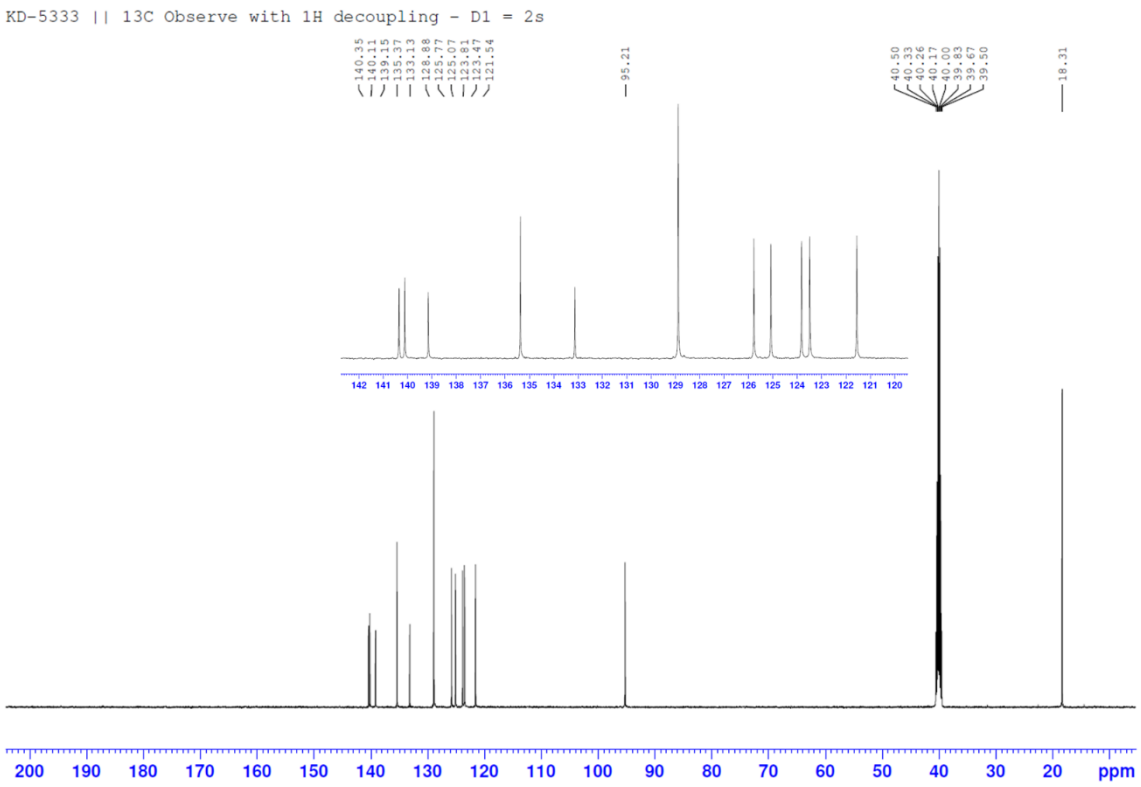

Fig. **S2**. ^{13}C NMR spectrum of **1** in DMSO-d_6.

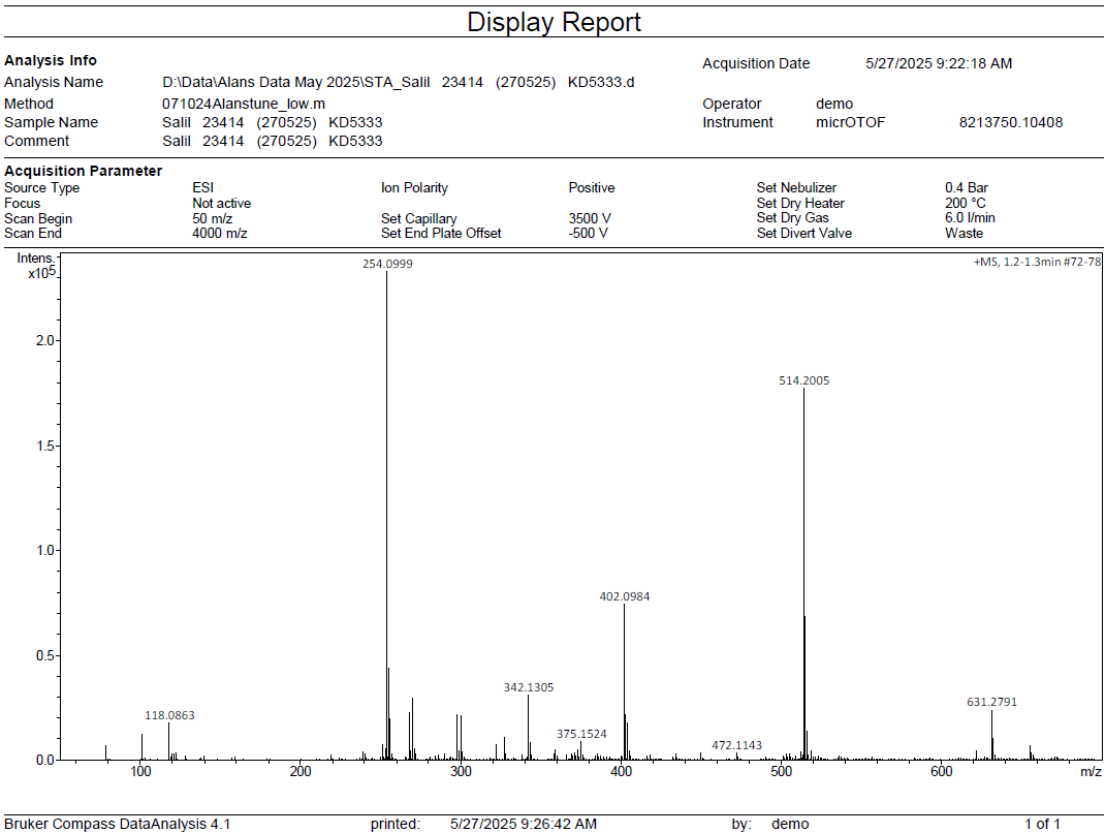

Fig. **S3**. HRMS of **1**.

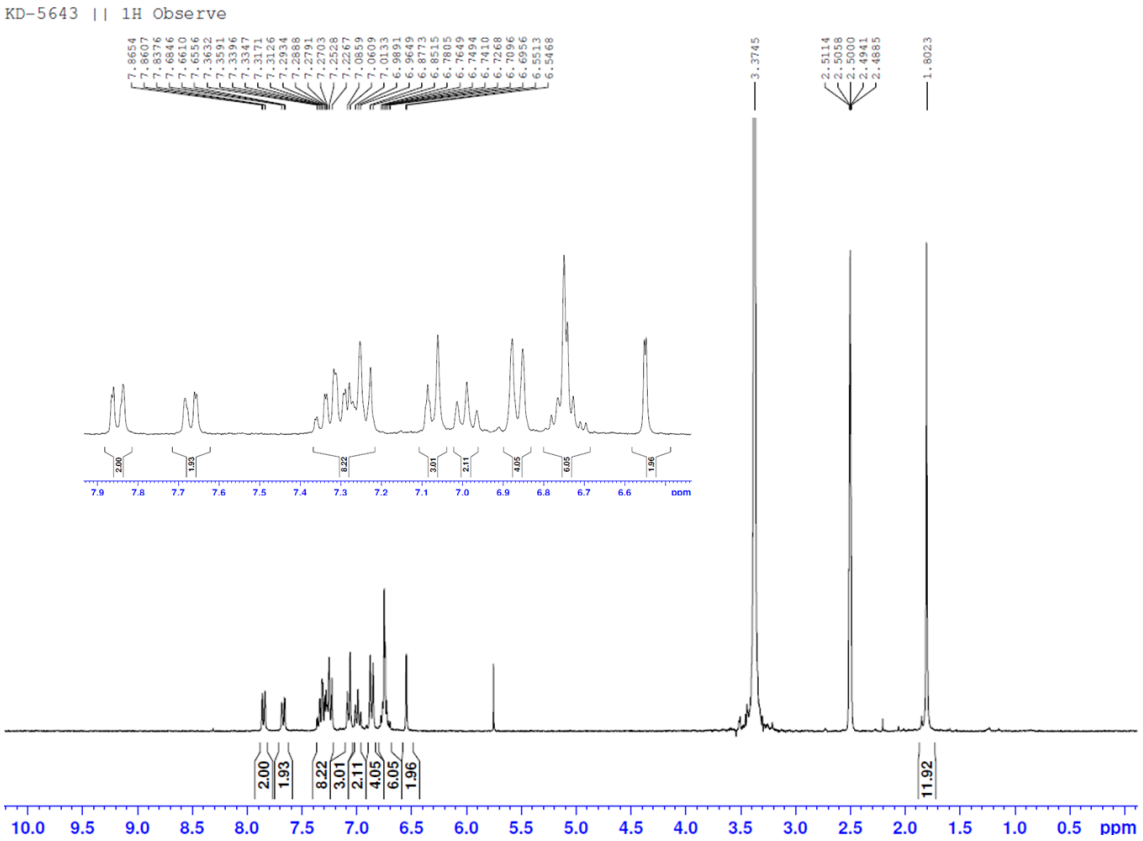

Fig. **S4**. ^{1}H NMR spectrum of **2** in DMSO-d_6.

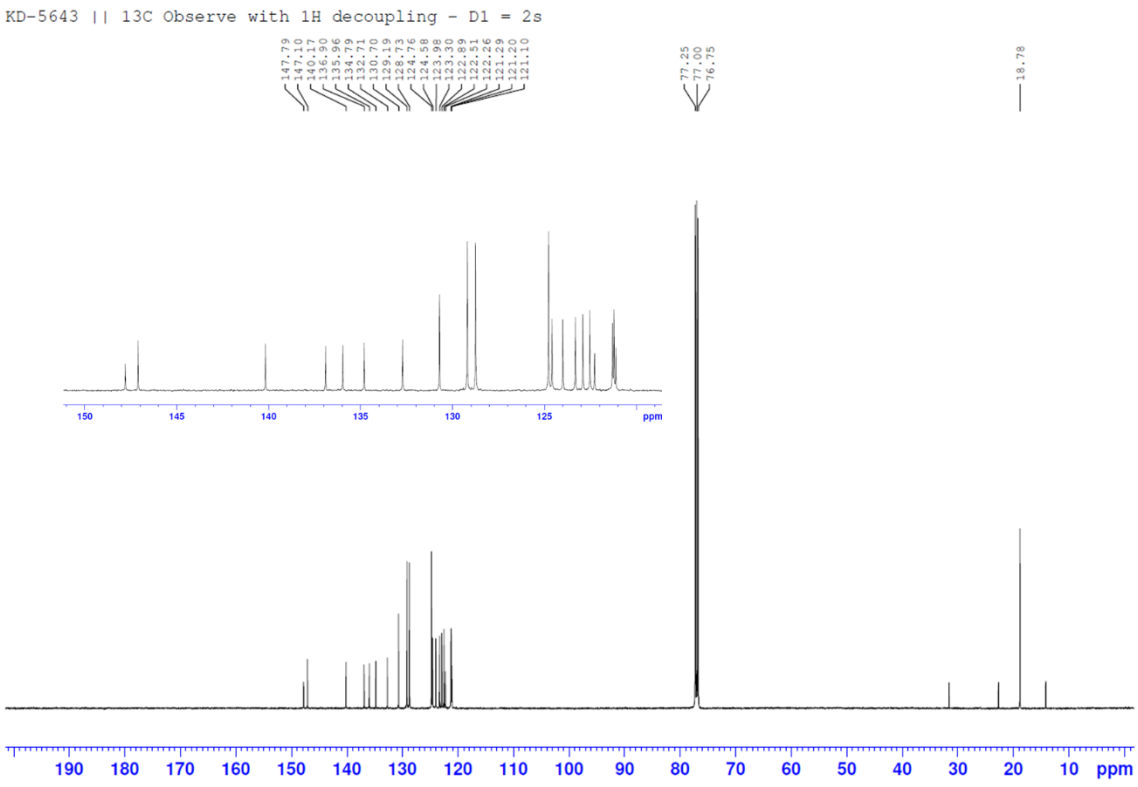

Fig. **S5**. ^{13}C NMR spectrum of **2** in $CDCl_3$.

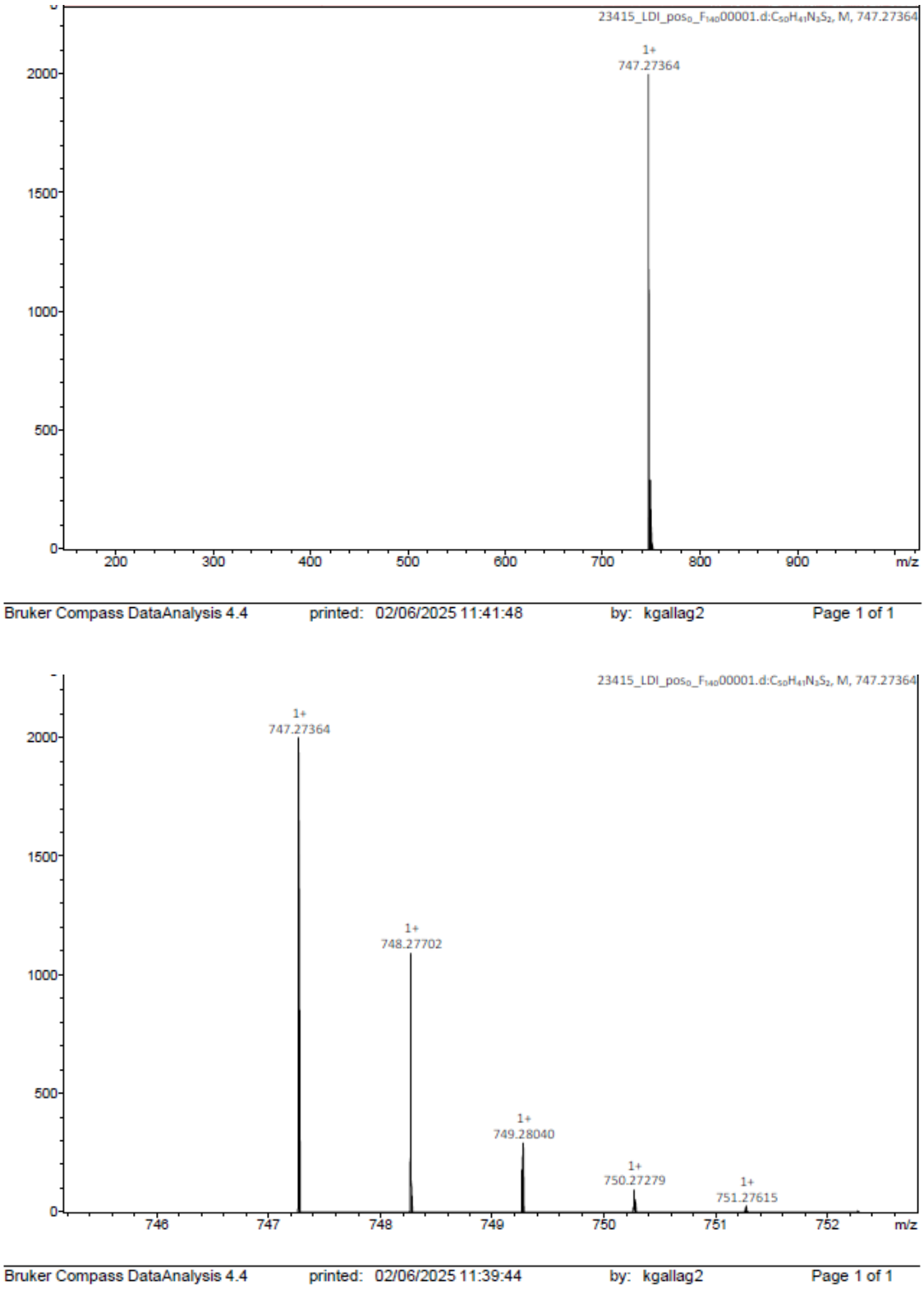

Fig. **S6**. HRMS of **2**. The peak at 747.27364 corresponds to $[C_{50}H_{41}N_3S_2 + H]^+$.

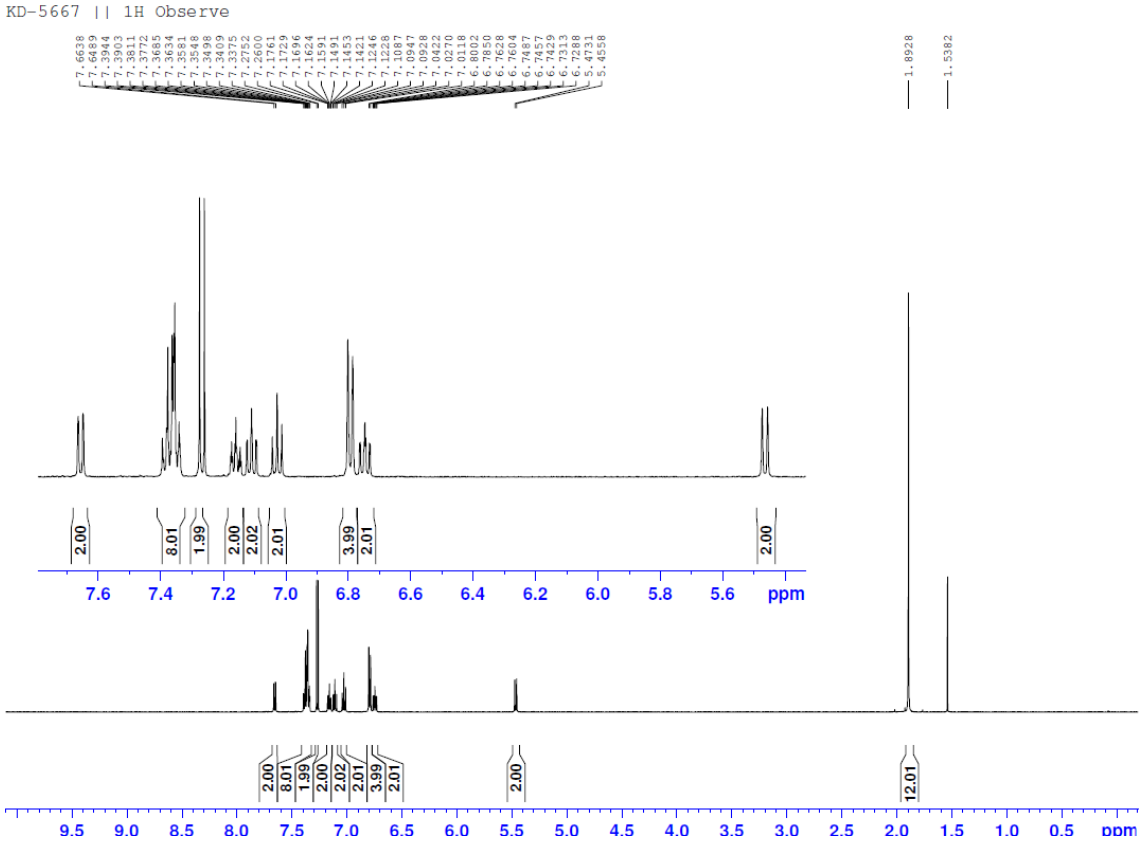

Fig. **S7**. ^{1}H NMR spectrum of **BT-DBIP** in $CDCl_3$.

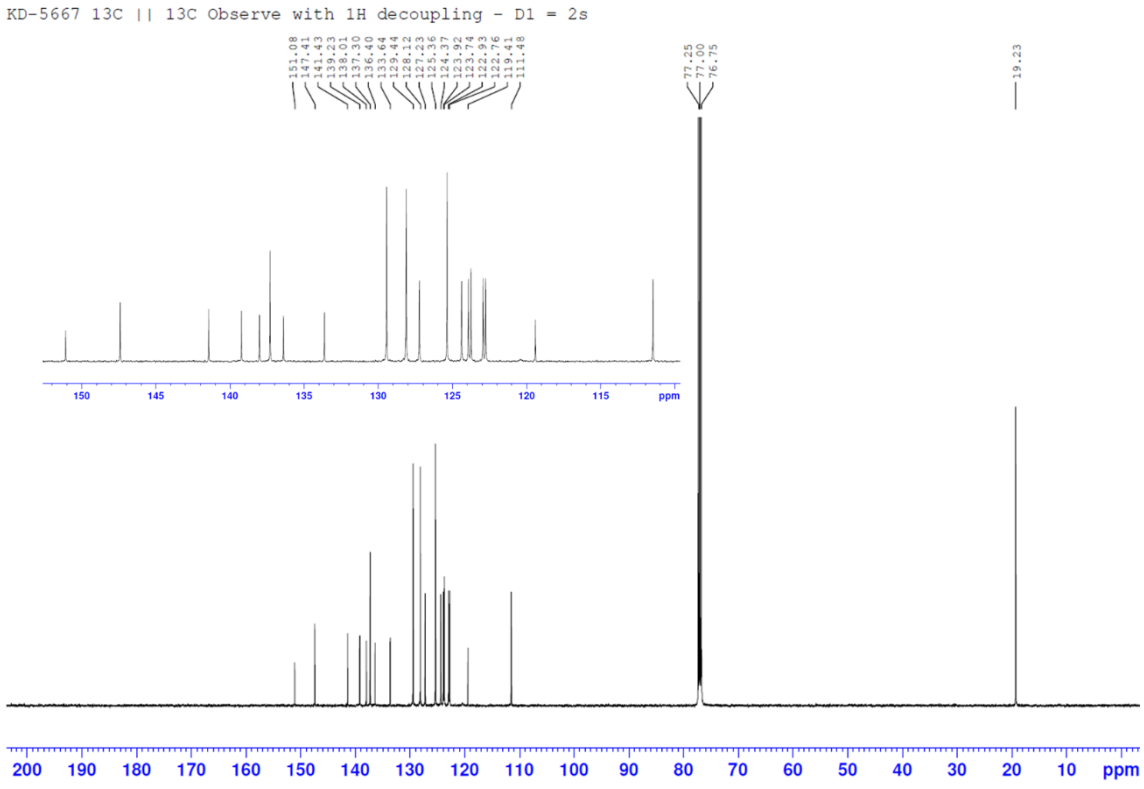

Fig. **S8**. ^{13}C NMR spectrum of **BT-DBIP** in $CDCl_3$.

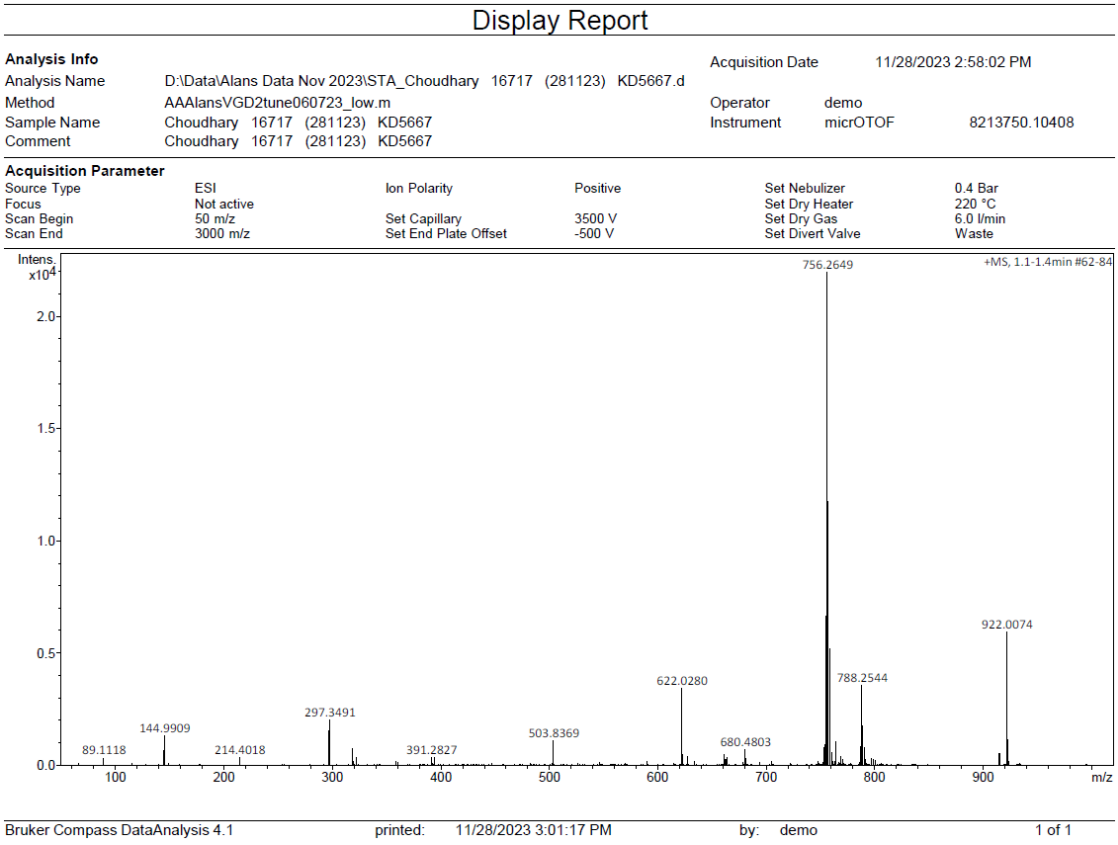

Fig. **S9**. HRMS of **BT-DBIP**. The peak at 756.2649 corresponds to $[C_{50}H_{38}BN_3S_2 + H]^+$.

LONDON METROPOLITAN UNIVERSITY
HUMAN SCIENCES

Elemental Analysis Sample Results

Name	Abhishek
Organisation Name	University of St Andrews
Purchase order number	P00032804

Standard – Acetanilide		
Element	**Expected %**	**Found**
Carbon	71.10 (+/- 0.23)	71.23
Hydrogen	6.71 (+/- 0.07)	6.71
Nitrogen	10.34 (+/- 0.09)	10.28

Analysis – KD-5667			
Element	**Expected %**	**Found (1)**	**Found (2)**
Carbon	79.46	78.70	78.56
Hydrogen	5.07	5.15	5.21
Nitrogen	5.56	5.18	5.24

Date completed	28.05.2025
Signature	O. McCullough
Comments	

Fig. **S10**. Elemental analysis of **BT-DBIP**.

<Sample Information>

Sample Name	: KD-5667		
Sample ID	:		
Method Filename	: 80% THF 20% water 0.6 mlmin 20 mins.lcm		
Batch Filename	: shut down.lcb		
Vial #	: 2-6	Sample Type	: Unknown
Injection Volume	: 10 uL		
Date Acquired	: 14/07/2023 12:24:42	Acquired by	: System Administrator
Date Processed	: 14/07/2023 12:44:44	Processed by	: System Administrator

<Chromatogram>

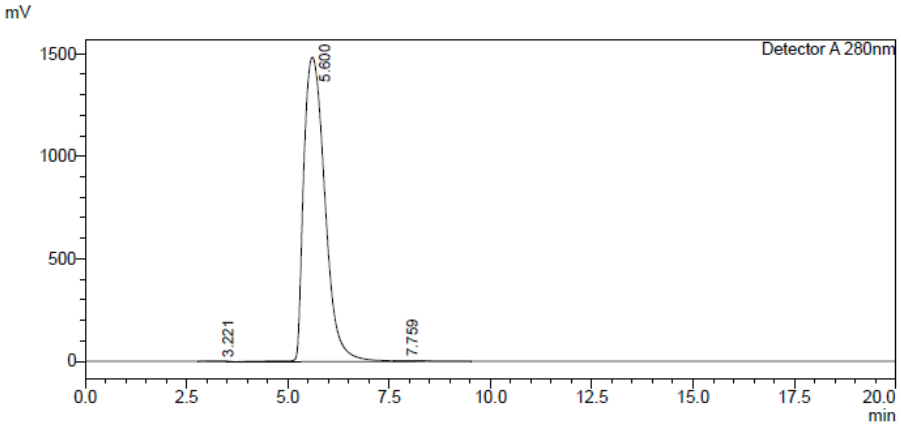

<Peak Table>

Detector A 280nm

Peak#	Ret. Time	Area	Height	Area%	Area/Height	Width at 5% Height
1	3.221	99209	2774	0.183	35.759	0.858
2	5.600	54197788	1485027	99.798	36.496	1.130
3	7.759	10275	406	0.019	25.289	0.602
Total		54307271	1488207	100.000		

Fig. **S11**. HPLC trace of **BT-DBIP**.

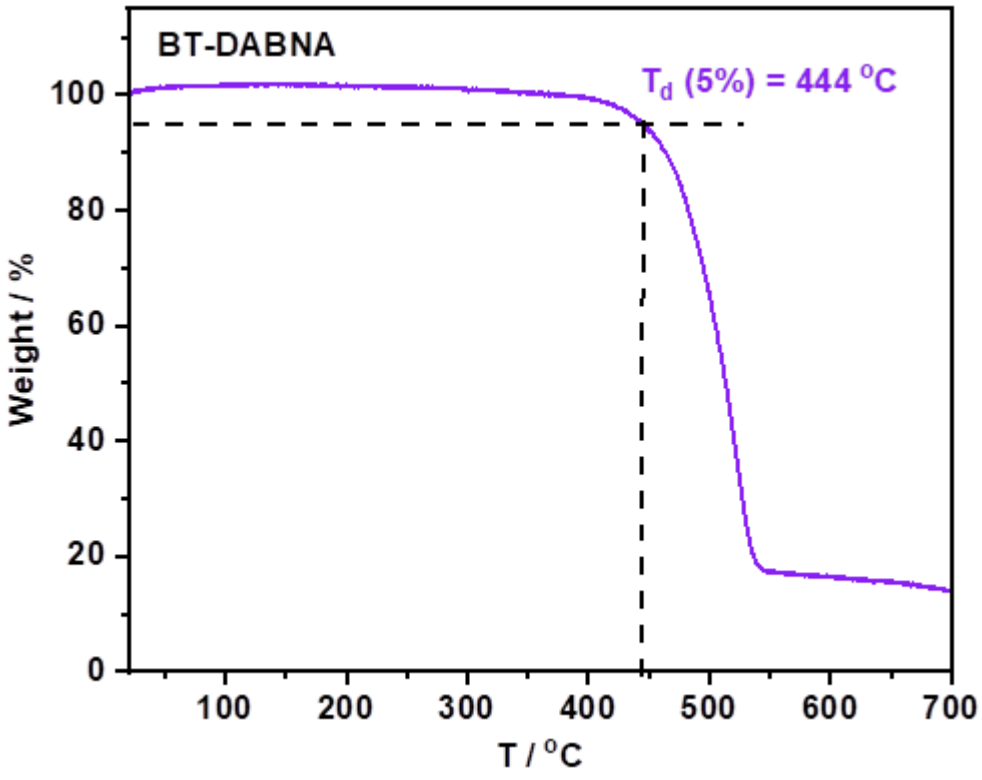

Fig. **S12**. TGA of **BT-DBIP**. The measurement was performed under a continuous N_2 flow and at a temperature ramp rate of 10 °C/min.

Calculations

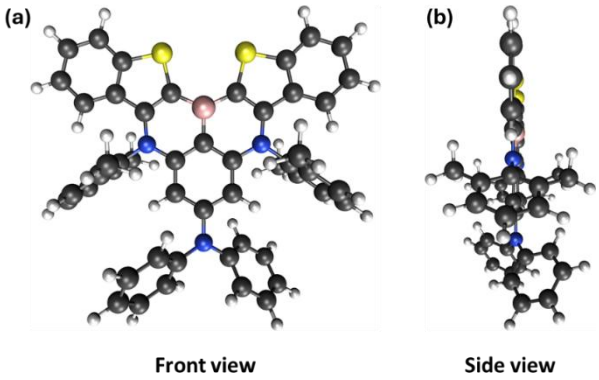

Fig. **S13**. Calculated optimized geometry of **BT-DBIP** at the PBE0/6-31G(d,p) level in the gas phase, (a) front view and (b) side view.

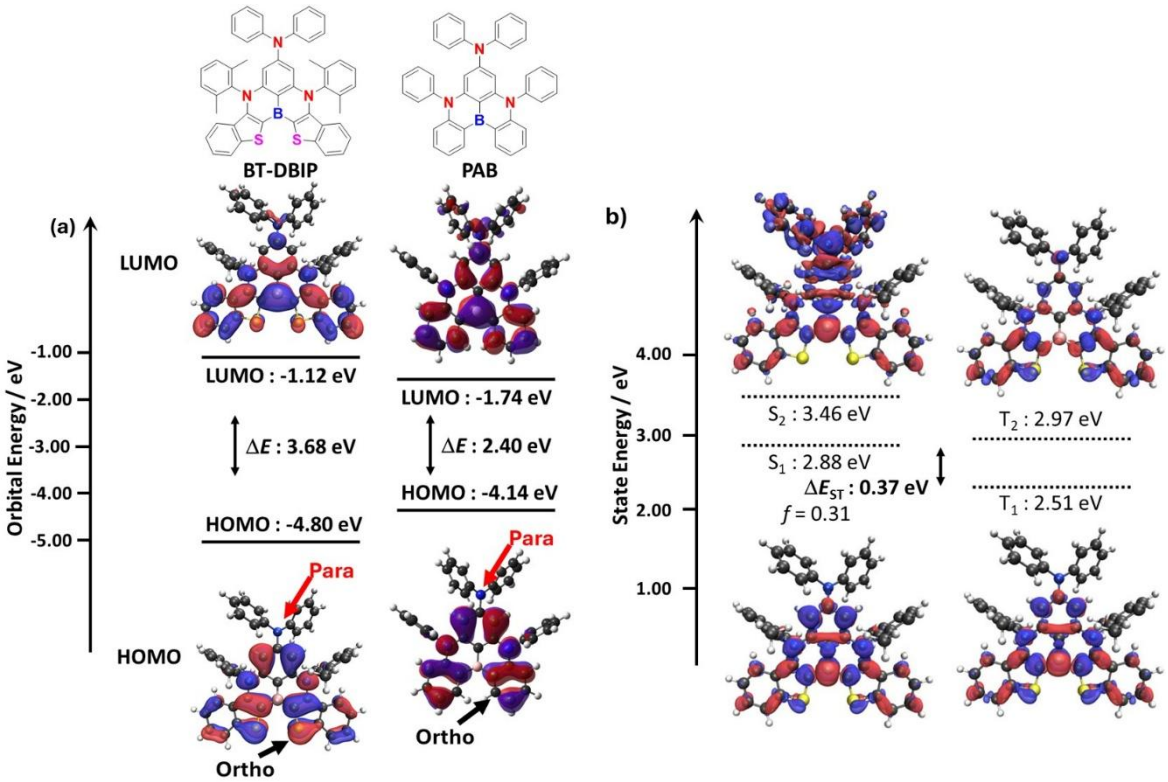

Fig. **S14**. a) Frontier orbitals of **BT-DBIP** and **PAB** (isovalue of 0.02) calculated at the PBE0/6-31G(d,p) level in the gas phase, b) difference density plots and energies for the two lowest lying singlet and triplet excited states for **BT-DBIP** calculated at SCS-CC2/cc-pVDZ in the gas phase (isovalue = 0.001). Blue color represents an area of decreased electron density and red represents an increased

electron density between the ground and excited states. *f* denotes the oscillator strength for the transition to the excited singlet state.

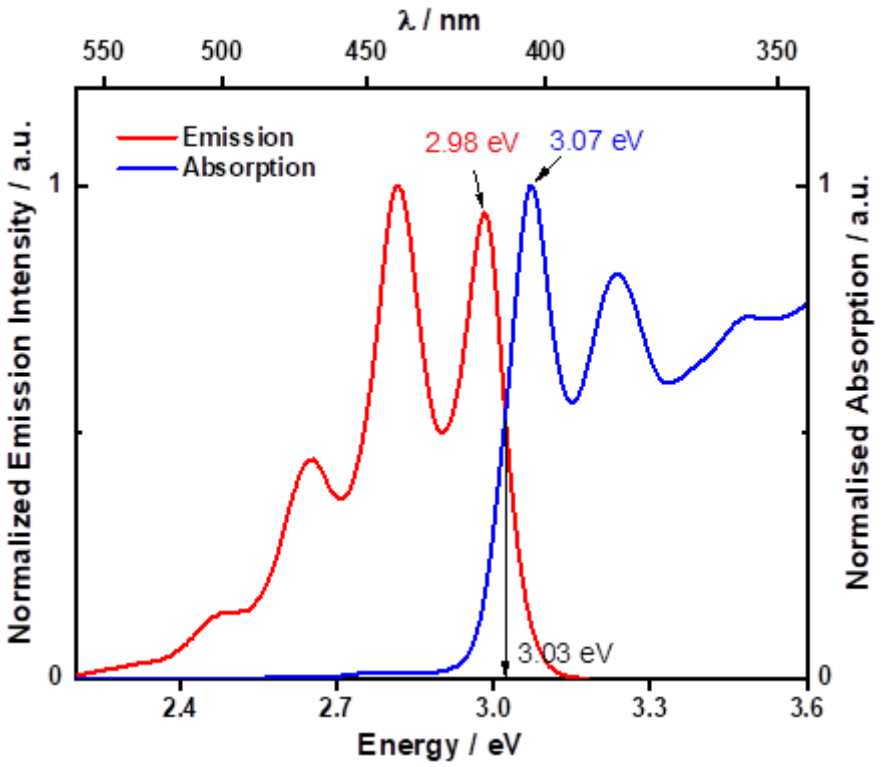

Fig. **S15**. Normalized absorption and emission spectra in toluene (λ_{exc} = 374 nm).

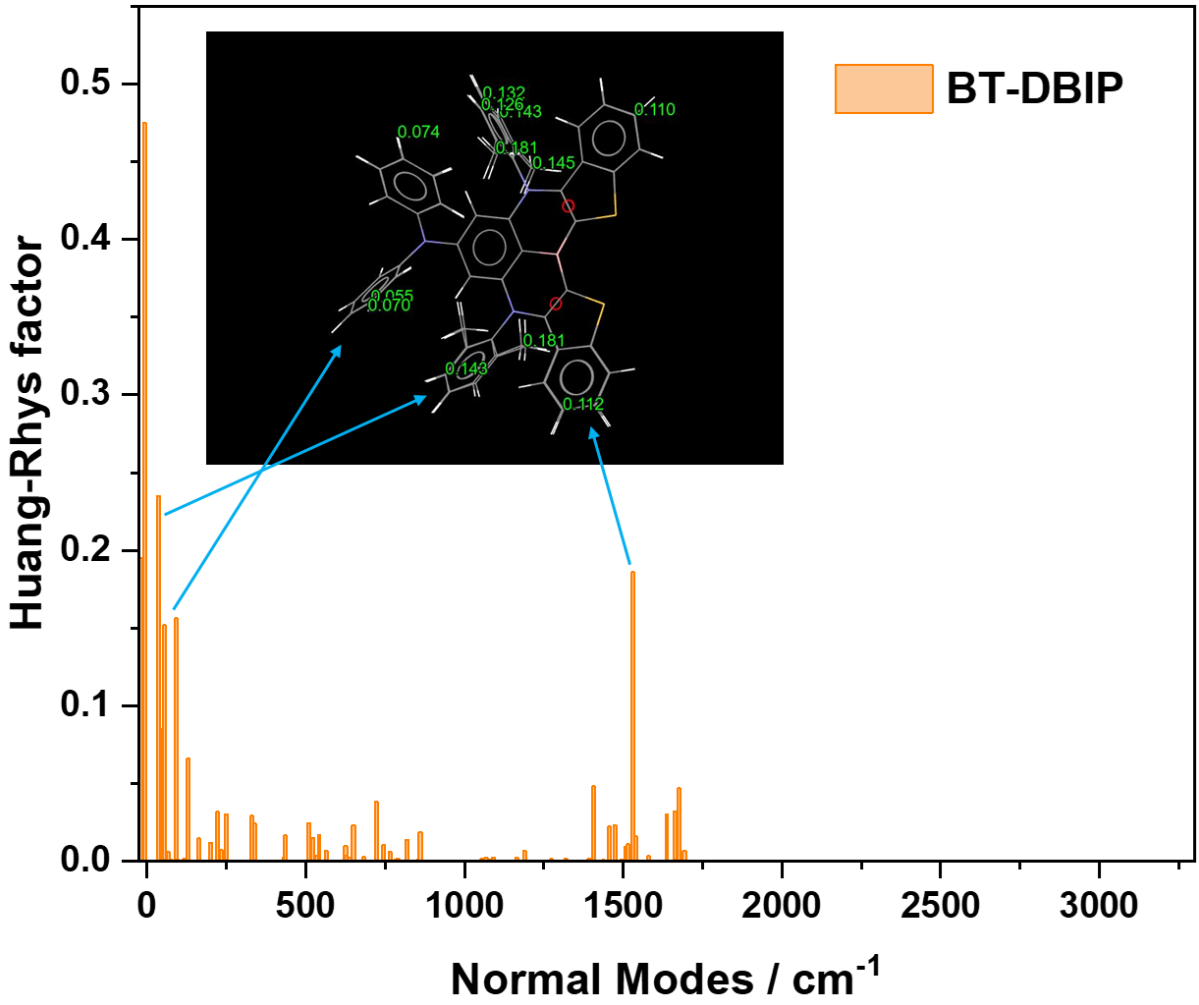

Fig. **S16**. The Huang–Rhys factor (HR) as a function of frequency under the representative vibration modes for S_1–S_0 transition of **BT-DBIP.** Inset figure belongs to merged ground (S_0) and excited state (S_1) molecular structures.

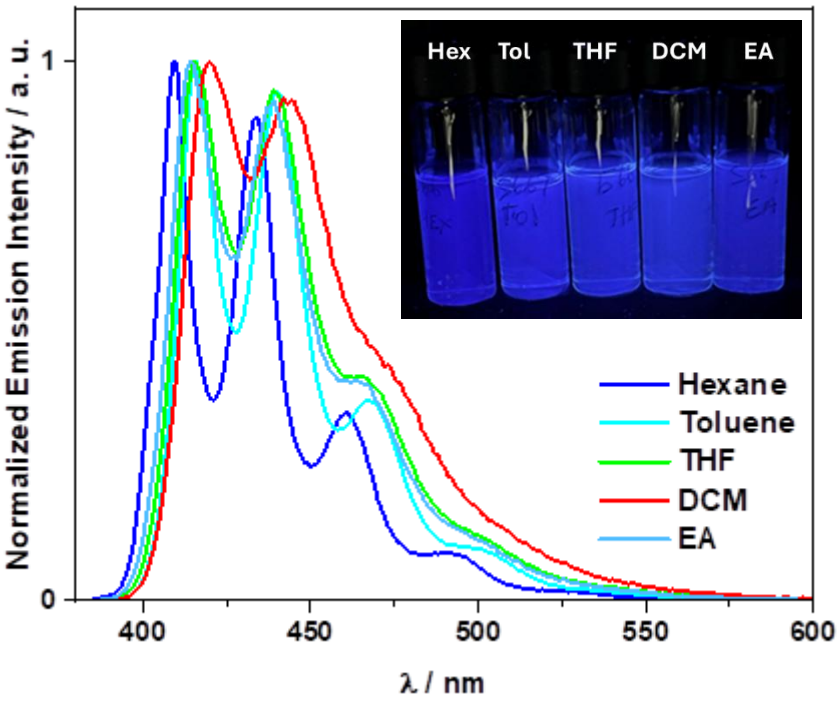

Fig. **S17**. PL Solvatochromism study of **BT-DBIP**, λ_{exc} = 374 nm.

Table **S1**. Photophysical properties of **BT-DBIP** in different solvents.[a]

Solvent	**BT-DBIP**	
	λ_{PL} / nm	**FWHM / nm**
Hex	409, 434	53
PhMe	416, 440	53
EtOAc	414, 439	55
THF	415, 439	54
DCM	420, 442	57

[a] λ_{exc} = 374 nm.

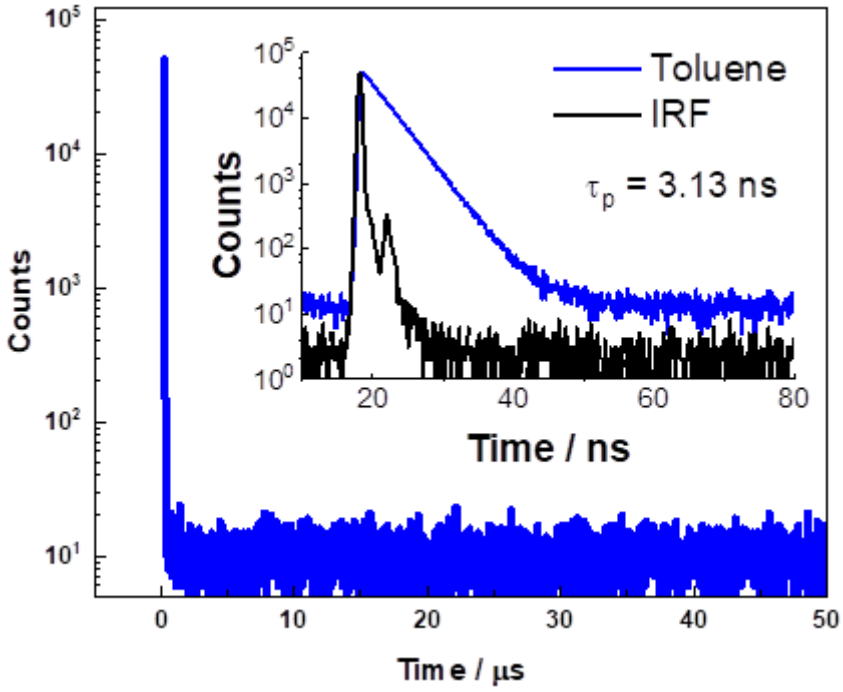

Fig. **S18**. Time-resolved PL decays by TCSPC of **BT-DBIP** measured in toluene solution at RT under vacuum for λ_{em} = 416 nm (λ_{exc} = 375 nm) (time window 0-50 μs). Inset, time-resolved PL decay of the prompt emission measured by TCSPC (time window 0-80 ns).

Table **S2**. TDA-DFT theoretical prediction of vertical excitation for **BT-DBIP** at the PBE0/6-31G(d,p) level in the gas phase.

Vertical excitation	λ_{emi} / nm	*f*	Transitions (Probability)
S_0 - S_1	395	0.33	HOMO → LUMO (0.95)
S_0 – S_2	356	0.17	HOMO-1 → LUMO (0.92)

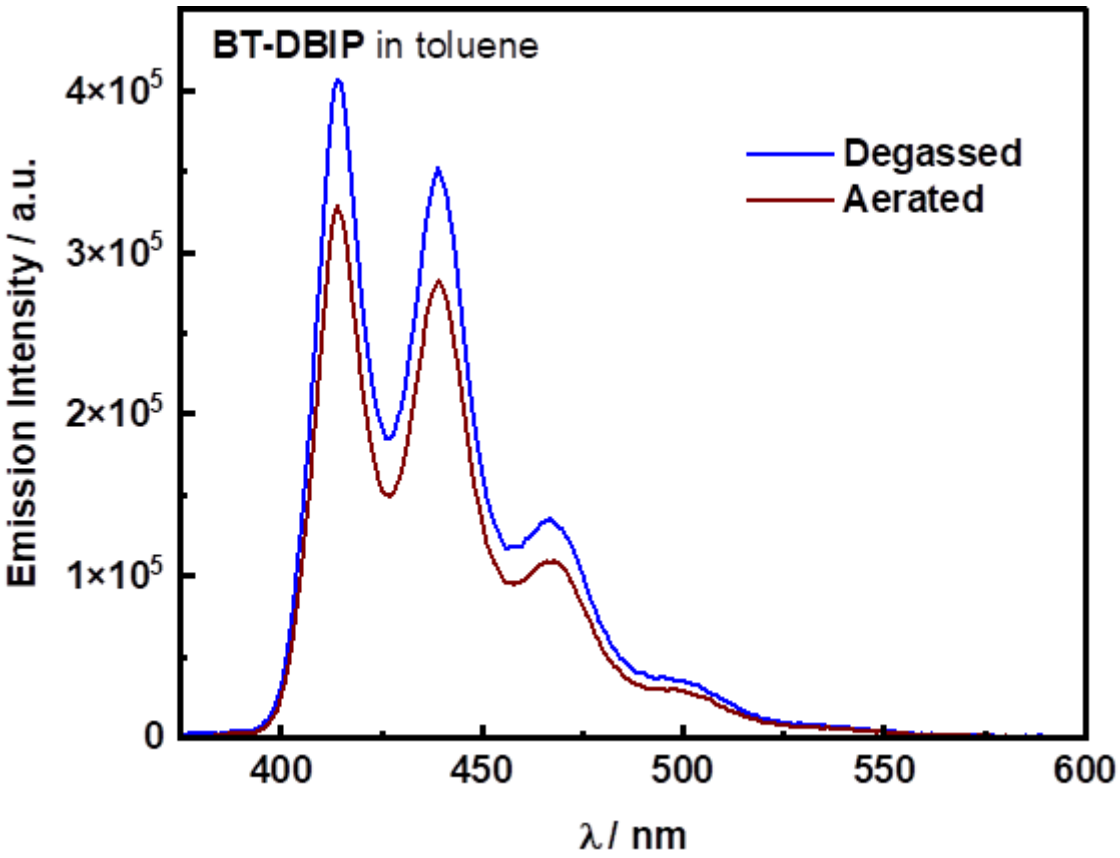

Fig. **S19**. Emission spectra of **BT-DBIP** in toluene solution with optical density 0.1 under aerated and degassed conditions (λ_{exc} = 347 nm).

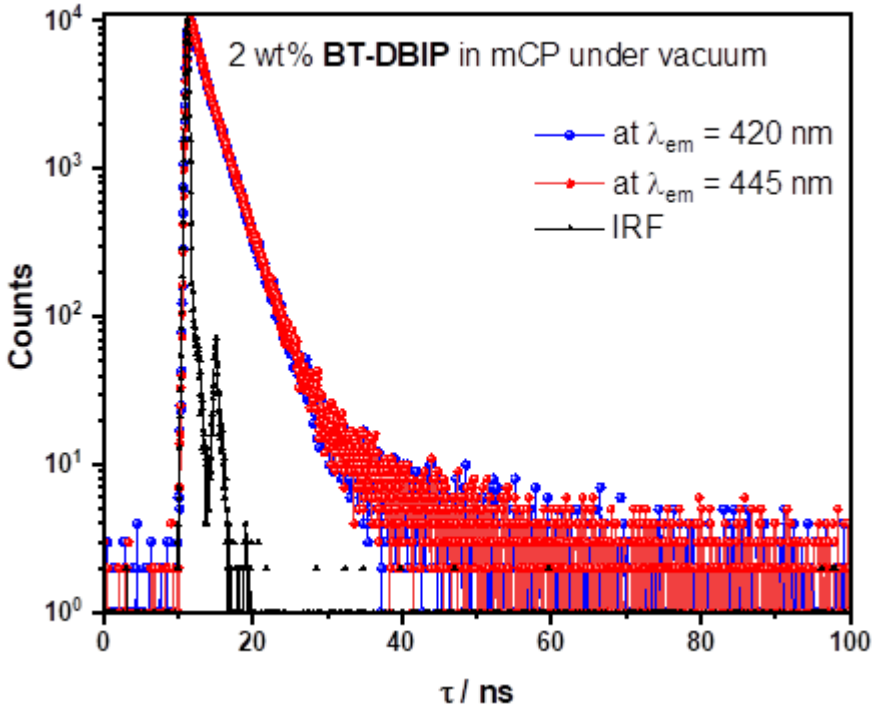

Fig. **S20**. Time-resolved PL decays measured by TCSPC of 2 wt% doped films of **BT-DBIP** in mCP for λ_{em} of 420 and 445 nm (λ_{exc} = 375 nm).

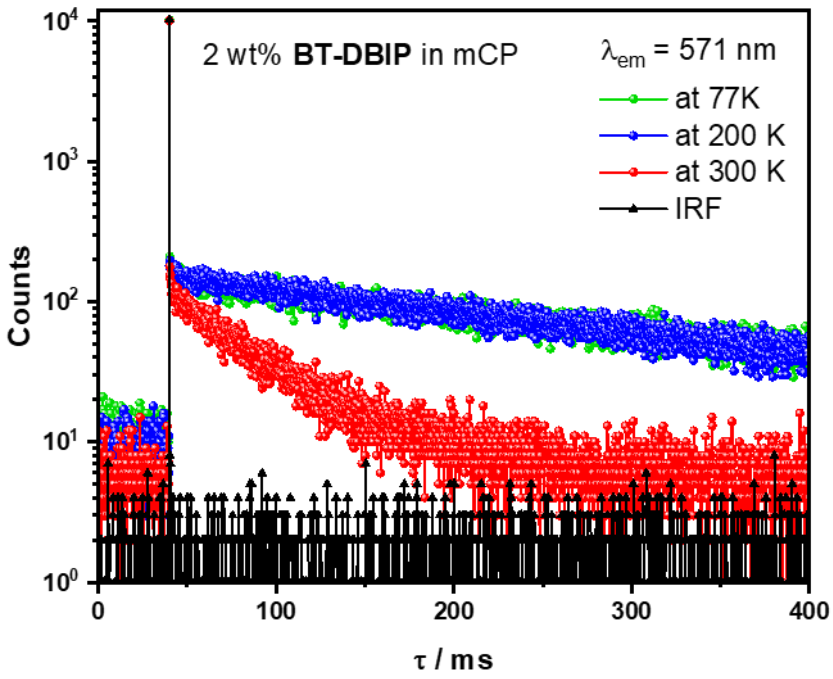

Fig. **S21**. Temperature-dependent time-resolved PL decays measured by MCS of 2 wt% doped films of **BT-DBIP** in mCP for λ_{Ph} = 571 nm. Film was excited by a microsecond flash lamp at λ_{exc} = 340 nm. IRF is the instrument response function.

References

1. G. A. Crosby and J. N. Demas, Measurement of photoluminescence quantum yields. Review, *J. Phy. Chem.*, 1971, **75**, 991-1024.
2. W. H. Melhuish, Quantum efficiencies of fluorescence of organic substances: Effect of solvent and concentration of the fluorescent solute1, *J. Phy. Chem* , 1961, **65**, 229-235.
3. A. M. Brouwer, Standards for photoluminescence quantum yield measurements in solution (IUPAC Technical Report), *Pure Appl. Chem*., 2011, **83**, 2213-2228.
4. J. Pommerehne, H. Vestweber, W. Guss, R. F. Mahrt, H. Bässler, M. Porsch and J. Daub, Efficient two layer leds on a polymer blend basis, *Adv. Mater.*, 1995, **7**, 551-554.
5. C. M. Cardona, W. Li, A. E. Kaifer, D. Stockdale and G. C. Bazan, Electrochemical Considerations for Determining Absolute Frontier Orbital Energy Levels of Conjugated Polymers for Solar Cell Applications, *Adv. Mater* , 2011, **23**, 2367-2371.
6. M. J. Frisch, G. W. Trucks, H. B. Schlegel, G. E. Scuseria, M. A. Robb, J. R. Cheeseman, G. Scalmani, V. Barone, G. A. Petersson, H. Nakatsuji, X. Li, M. Caricato, A. V. Marenich, J. Bloino, B. G. Janesko, R. Gomperts, B. Mennucci, H. P. Hratchian, J. V. Ortiz, A. F. Izmaylov, J. L. Sonnenberg, Williams, F. Ding, F. Lipparini, F. Egidi, J. Goings, B. Peng, A. Petrone, T. Henderson, D. Ranasinghe, V. G. Zakrzewski, J. Gao, N. Rega, G. Zheng, W. Liang, M. Hada, M. Ehara, K. Toyota, R. Fukuda, J. Hasegawa, M. Ishida, T. Nakajima, Y. Honda, O. Kitao, H. Nakai, T. Vreven, K. Throssell, J. A. Montgomery Jr., J. E. Peralta, F. Ogliaro, M. J. Bearpark, J. J. Heyd, E. N. Brothers, K. N. Kudin, V. N. Staroverov, T. A. Keith, R. Kobayashi, J. Normand, K. Raghavachari, A. P. Rendell, J. C. Burant, S. S. Iyengar, J. Tomasi, M. Cossi, J. M. Millam, M. Klene, C. Adamo, R. Cammi, J. W. Ochterski, R. L. Martin, K. Morokuma, O. Farkas, J. B. Foresman and D. J. Fox, Gaussian, Inc., Wallingford CT, 2016.
7. C. Adamo and V. Barone, Toward reliable density functional methods without adjustable parameters: The PBE0 model, *J. Chem. Phy.*, 1999, **110**, 6158-6170.
8. T. H. Dunning, Jr., Gaussian basis sets for use in correlated molecular calculations. I. The atoms boron through neon and hydrogen, *J. Chem. Phy* , 1989, **90**, 1007-1023.

9. S. Grimme, Density functional calculations with configuration interaction for the excited states of molecules, *Chem. Phy. Lett.*, 1996, **259**, 128-137.

10. S. Hirata and M. Head-Gordon, Time-dependent density functional theory within the Tamm–Dancoff approximation, *Chem. Phy. Lett* , 1999, **314**, 291-299.

11. T. A. K. Roy Dennington, and John M. Millam, Semichem Inc., Shawnee Mission, KS, 2016.

12. O. S. Lee and E. Zysman-Colman. Silico(version 0.18), 2020.

13. O. S. Lee, M. C. Gather and E. Zysman-Colman, Digichem: computational chemistry for everyone, *Digital Discovery*, 2024, **3**, 1695-1713.

14. N. M. O'boyle, A. L. Tenderholt and K. M. Langner, cclib: A library for package-independent computational chemistry algorithms, *J. Comput. Chem.*, 2008, **29**, 839-845.

15. W. Humphrey, A. Dalke and K. Schulten, VMD: Visual molecular dynamics, *J. Mol. Graph.*, 1996, **14**, 33-38.

16. J . Stone, Computer Science Department, University of Missouri-Rolla, 1998.

17. J. D. Hunter, Matplotlib: A 2D Graphics Environment, *Comput. Sci. Eng.*, 2007, **9**. 90-95.

18. N. M. O'Boyle, M. Banck, C. A. James, C. Morley, T. Vandermeersch and G. R. Hutchison, 1Open Babel: An open chemical toolbox, *J. Cheminform*. 2011, **3**, 33.

19. N. M. O'Boyle and G. R. Hutchison, Cinfony – combining Open Source cheminformatics toolkits behind a common interface, *Chem. Cent. J.*, 2008, **2**, 24.

20. X. Gao, S. Bai, D. Fazzi, T. Niehaus, M. Barbatti and W. Thiel, Evaluation of Spin-Orbit Couplings with Linear-Response Time-Dependent Density Functional Methods, *J. Theory Comput.*, 2017, **13**, 515-524.

21. J. R. Reimers, A practical method for the use of curvilinear coordinates in calculations of normal-mode-projected displacements and Duschinsky rotation matrices for large molecules, *J. Chem. Phy.*, 2001, **115**, 9103-9109.